Health status and resonance in a model for living organisms under periodic stress and healing

B.-G. Yoon,[1,*] J. Choi,[2] M. Y. Choi,[3,4] and J.-Y. Fortin[5]
[1]*Department of Physics, University of Ulsan, Ulsan 680-749, Korea*
[2]*Department of Physics, Keimyung University, Daegu 704-701, Korea*
[3]*Department of Physics and Center for Theoretical Physics, Seoul National University, Seoul 151-747, Korea*
[4]*Korea Institute for Advanced Study, Seoul 130-722, Korea*
[5]*Laboratoire de Physique Théorique, Université Louis Pasteur, 67084 Strasbourg, France*
(Received 25 July 2005; revised manuscript received 7 December 2005; published 7 March 2006)

We apply the dynamic model for failures to a living organism under periodic stress and study how the health status of the organism evolves. It is found that without healing, the average fraction of intact cells decays either stepwise to zero or to a constant value far from zero, depending on the peak value of the periodic stress. As the parameter measuring the healing probability is raised from zero, the fraction exhibits oscillating behavior, reminiscent of periodic synchronization. The power spectrum at the stress frequency at first increases with the healing parameter, then decreases, which may be called healing resonance. We also study the time evolution of the system in the case that the healing parameter varies periodically with time and observe a transition from the unhealthy state to the healthy one as the healing frequency increases. This suggests how to adjust the frequency of medical treatment to the optimum.

DOI: 10.1103/PhysRevE.73.031905 PACS number(s): 87.10.+e, 05.40.−a, 87.18.Bb

I. INTRODUCTION

Biological systems, consisting of cells, may be led into failures, for example, as a consequence of disease. Under the stress due to such an external load, some of the cells may fail or die and the corresponding extra stress, previously handled by those (now failed) cells, should be transferred to other (intact) cells. This gives rise to an increase of the stress on the remaining cells and may in turn induce additional failures of cells. In this manner local stress arising from an external load tends to produce avalanches of cell failures, possibly resulting in the failure of the whole system. On the other hand, there may also exist an ability to heal: Failed cells may be repaired or new cells may be regenerated in the place of failed ones. Such an ability to heal, as a characteristic of biological systems, makes a distinction from breakdown phenomena in other systems, described by fiber bundle models [1–3].

These features are incorporated in the recently proposed dynamic model for failures, which exhibits many desirable properties as to the evolution to the stationary state and the lifetime under a given applied stress [4]. For example, the dynamic model gives a characteristic time evolution that the system tends to resist stress for a rather long time, followed by a sudden failure with some fraction of cells surviving; this is called the "unhealthy" state. If such breakdown does not occur, the state is regarded as "healthy." It also shows that the critical stress beyond which the system breaks down increases rapidly as the healing ability is introduced, indicative of the importance of healing in biological systems. With these features, the model gives a good description of the time course of degenerative disease progression such as diabetes [5], Alzheimer's disease [6], and possibly AIDS [7] and might be used as a starting point to understand failure phenomena in pathology. Here an interesting application of the model would be to study the effects of time-varying stress, to which living organisms are usually subject. Of particular interest is the case of periodic stress, in view of the environments or external doses changing with periods of, for example, a day or a year.

This paper studies the behavior of a living organism under periodic stress through the use of the dynamic model for failures. We introduce the healing parameter, which measures the cell regeneration ability, and examine the behavior as the healing parameter is varied. In the absence of healing, the average fraction of intact cells is found to decay stepwise either to zero or to a constant value far from zero, depending on the peak value of the periodic stress. When the healing parameter is raised from zero, the fraction exhibits oscillating behavior, which is reminiscent of periodic synchronization. The power spectrum at the stress frequency at first increases with the healing parameter, then decreases, manifesting resonance behavior. We also study the time evolution of the system in the case that the healing parameter varies periodically with time; observed is a transition from the unhealthy state to the healthy one as the healing frequency increases. This gives an interesting criterion of adjusting the frequency of medical treatment to the optimum.

This paper consists of five sections: Section II describes briefly the dynamic model for failures for completeness. In Sec. III we integrate numerically the equation of motion with periodic stress and compute corresponding power spectra, whereas Sec. IV presents the interplay between stress and healing and discusses its implication for medication. Finally, a summary is given in Sec. V.

II. DYNAMIC MODEL FOR FAILURES

We consider an organism consisting of N cells under external stress characterized by load F which may vary with

*Author to whom correspondence should be addressed. Electronic address: bgyoon@ulsan.ac.kr

time t. Each cell has its own threshold and endures stress below the threshold. The cell may become dead, however, if the threshold is exceeded. We assign "spin" variables to these in such a way that $s_i=-1(+1)$ for the ith cell alive (dead). The state of the organism is then described by the configuration of all the cells, $\mathbf{s}\equiv(s_1,s_2,\ldots,s_N)$. The total number N_- of alive cells is related with the average spin $\bar{s}\equiv N^{-1}\Sigma_j s_j$ via

$$N_- = \sum_{j=1}^{N} \frac{1-s_j}{2} = \frac{N}{2}(1-\bar{s}), \tag{1}$$

and we are interested in how N_- evolves in time as well as its stationary value. The total stress on the ith cell can then be written in the form

$$\eta_i = f + \sum_j V_{ij}\frac{1+s_j}{2}, \tag{2}$$

where $f=F/N$ is the direct stress due to the external load and V_{ij} represents the stress transferred from the jth cell (in case that it is dead). The breaking of the ith cell with tolerance h_i is determined according to

$$\eta_i < h_i \Rightarrow s_i = -1, \quad \eta_i > h_i \Rightarrow s_i = +1,$$

which, in terms of the local field $E_i(\mathbf{s})\equiv(\eta_i-h_i)(1-\bar{s})/2$, can be simplified as

$$s_i E_i > 0. \tag{3}$$

This determines the stationary configuration at which the organism eventually arrives.

For a more realistic description of the time evolution, we also take into consideration the uncertainty ("noise") present in real situations, which may arise from imperfections, random variations, and other environmental influences. We thus begin with the conditional probability that the ith cell is dead at time $t+\delta t$, given that it is alive at time t:

$$p(s_i=+1,t+\delta t|s_i=-1,t;\mathbf{s}',t-t_d) = \frac{\delta t}{2t_r}[1+\tanh\beta E_i'], \tag{4}$$

where $\mathbf{s}'\equiv(s_1',s_2',\ldots,s_N')$ represents the configuration of the organism at time $t-t_d$ and $E_i'\equiv E_i(\mathbf{s}')$ is the local field at time $t-t_d$. Note the two time scales t_d and t_r here: t_d denotes the time delay during which the stress is redistributed among cells while the refractory period t_r sets the relaxation time (or lifetime). The "temperature" $T\equiv\beta^{-1}$ measures the width of the threshold region of the cells or the noise level: In the noiseless limit ($T=0$) the factor $(1+\tanh\beta E_i')/2$ in Eq. (4) reduces to the step function $\theta(E_i')$, yielding the stationary-state condition given by Eq. (3). We also assign the nonzero conditional probability of the ith cell being repaired (or regenerated) given that it is dead at time t, according to

$$p(s_i=-1,t+\delta t|s_i=+1,t;\mathbf{s}',t-t_d) = \frac{\delta t}{t_0}, \tag{5}$$

where t_0 is the time necessary for cell regeneration. Equations (4) and (5) can be combined to give a general expression for the conditional probability $p(s_i',t+\delta t|s_i,t;\mathbf{s}',t-t_d)$, which, in the limit $\delta t\to 0$, can be expressed in terms of the transition rate:

$$p(-s_i,t+\delta t|s_i,t;\mathbf{s}',t-t_d) = w_i(s_i;\mathbf{s}',t-t_d)\,\delta t. \tag{6}$$

The transition rate is given by

$$w_i(s_i;\mathbf{s}',t-t_d) = \frac{1}{2t_r}\left[\left(a+\frac{1}{2}\right)+\left(a-\frac{1}{2}\right)s_i+\frac{1-s_i}{2}\tanh\beta E_i'\right], \tag{7}$$

where the healing parameter $a\equiv t_r/t_0$ measures the regeneration probability during the relaxation time.

The behavior of the organism is then governed by the master equation, which describes the evolution of the joint probability $P(\mathbf{s},t;\mathbf{s}',t-t_d)$ that the organism is in state $\mathbf{s}'$ at time $t-t_d$ and in state $\mathbf{s}$ at time t:

$$\begin{aligned} P(\mathbf{s},t+\delta t;\mathbf{s}',t-t_d) - P(\mathbf{s},t;\mathbf{s}',t-t_d) \\ = -\sum_{\mathbf{s}''}[p(\mathbf{s}'',t+\delta t|\mathbf{s},t;\mathbf{s}',t-t_d)P(\mathbf{s},t;\mathbf{s}',t-t_d) \\ - p(\mathbf{s},t+\delta t|\mathbf{s}'',t;\mathbf{s}',t-t_d)P(\mathbf{s}'',t;\mathbf{s}',t-t_d)]. \end{aligned} \tag{8}$$

Thus we obtain the equation of motion in the form of a non-Markov master equation. Here the conditional probability for the whole organism is given by the product of that for each cell:

$$p(\mathbf{s}'',t+\delta t|\mathbf{s},t;\mathbf{s}',t-t_d) = \prod_{i=1}^{N} p(s_i'',t+\delta t|s_i,t;\mathbf{s}',t-t_d).$$

In the limit $\delta t\to 0$, Eq. (8) takes the differential form

$$\begin{aligned} \frac{d}{dt}P(\mathbf{s},t;\mathbf{s}',t-1) = -\sum_i [w_i(s_i;\mathbf{s}')P(\mathbf{s},t;\mathbf{s}',t-1) \\ - w_i(-s_i;\mathbf{s}')P(F_i\mathbf{s},t;\mathbf{s}',t-1)], \end{aligned} \tag{9}$$

where time t has been rescaled in units of the delay time t_d, the transition rate is given by $w_i(s_i;\mathbf{s}')\equiv t_d w_i(s_i;\mathbf{s}',t-t_d)$ with $w_i(s_i;\mathbf{s}',t-t_d)$ defined in Eq. (7), and $F_i\mathbf{s}\equiv(s_1,s_2,\ldots,-s_i,s_{i+1},\ldots,s_N)$. Note that only those contributions of intermediate configurations $\mathbf{s}'$ differing from $\mathbf{s}$ just by one cell are retained; other configurations give higher-order contributions, which vanish in the limit $\delta t\to 0$. Then equations describing the time evolution of the relevant physical quantities in general assume the form of differential-difference equations due to the retardation in the stress redistribution. In particular, the average spin for the kth cell, $m_k(t)\equiv\langle s_k\rangle \equiv\Sigma_{\mathbf{s},\mathbf{s}'}s_k P(\mathbf{s},t;\mathbf{s}',t-1)$, can be obtained from Eq. (9) by multiplying s_k and summing over all configurations:

$$\frac{d}{dt}m_k(t) = -2\langle s_k w_k(s_k;\mathbf{s}')\rangle, \tag{10}$$

where $\langle\ \rangle$ denotes the average over $P(\mathbf{s},t;\mathbf{s}',t-1)$. Evaluation of the average $\langle s_k w_k(s_k;\mathbf{s}')\rangle$, with $s_k^2=1$ noted, leads to

$$\tau\frac{d}{dt}m_k = \left(\frac{1}{2}-a\right) - \left(\frac{1}{2}+a\right)m_k + \left\langle \frac{1-s_k}{2}\tanh \beta E_k' \right\rangle, \tag{11}$$

where $\tau \equiv t_r/t_d$ gives the relaxation time (in units of t_d).

To proceed further, we consider global load sharing (GLS)—i.e., that the stress is distributed to every cell uniformly, leaving the case of local load sharing (LLS) to the end of Sec. III. In the case of GLS, we have $V_{ij}=\eta_j/N_-$ and, accordingly, $(1-\bar{s})\eta_i=2f$ from Eq. (2). The infinite-range nature of GLS allows one to replace E_k' by its average $\langle E_k'\rangle = f-(h_k/2)[1-\bar{m}(t-1)]$, where it has been noted that s' is the configuration at time $t-1$—i.e., $\langle \bar{s}'\rangle = N^{-1}\Sigma_j\langle \bar{s}_j'\rangle = N^{-1}\Sigma_j m_j(t-1) \equiv \bar{m}(t-1)$. For convenience, we now rewrite Eq. (11) in terms of the average number of living cells at time t. Defining the average living fraction $x_k \equiv (1-m_k)/2$ and the *health status* $\bar{x} \equiv N^{-1}\Sigma_k x_k = (1-\bar{m})/2$, we have, from Eq. (1), $\langle N_-\rangle = N\bar{x}$ and thus obtain from Eq. (11) the equation of motion for the average living fraction for the kth cell:

$$\tau\frac{d}{dt}x_k(t) = a - \left(\frac{1}{2}+a\right)x_k(t) - \frac{1}{2}x_k(t)\tanh \beta[f - h_k\bar{x}(t-1)], \tag{12}$$

which is analyzed in the next section.

III. PERIODIC STRESS

We first describe the mechanism how the organism reaches its stationary state under constant (direct) stress. In the noiseless limit ($T=0$), to which this work is devoted for simplicity, we consider two cases according as f is greater than $h_k\bar{x}(t-1)$ or less and write Eq. (12) accordingly: When $f > h_k\bar{x}(t-1)$, the external stress on the cell k is so strong that it dies according to

$$\tau\frac{d}{dt}x_k(t) = a - (1+a)x_k(t), \tag{13}$$

which yields the solution for the *dying* process:

$$x_k(t) = \frac{a}{1+a} + \left[x_k(t_0) - \frac{a}{1+a}\right]e^{-(1+a)(t-t_0)/\tau}. \tag{14}$$

Note that in the presence of healing ($a \neq 0$) the cell may not become completely dead on the average. Namely, some of the N cells in the organism may still survive, giving a nonzero value of the average living fraction ($x_k \neq 0$). In the real situation, however, the healing parameter a is not constant but dependent on, e.g., the fraction of living cells. Namely, it is likely that a reduces to zero as x_k decreases below a certain value. This point will be further elaborated on at the end of this section in such a way that the healing parameter a depends on the health status. For the moment, however, we concentrate on the case of constant a for simplicity.

On the other hand, in case that $f < h_k\bar{x}(t-1)$, Eq. (12) reads

$$\tau\frac{d}{dt}x_k(t) = a - ax_k(t), \tag{15}$$

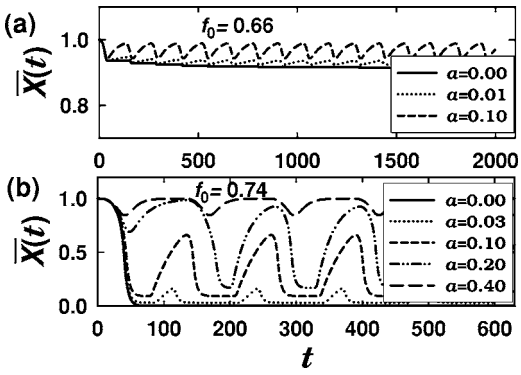

FIG. 1. The average fraction $\bar{x}$ of living cells versus time t (in units of the delay time) for several values of the healing parameter a. The organism is suffering the sinusoidal stress given by Eq. (17), with the peak stress f_0= (a) 0.66 and (b) 0.74 and period $\mathcal{T}=128$. There is no noise ($T=0$), and the values of tolerance h_i are distributed according to the Gaussian distribution with unit mean $\bar{h}=1$ and standard deviation $\sigma=0.2$.

which represents the cell *regeneration* process. The corresponding solution is given by

$$x_k(t) = 1 + [x_k(t_0) - 1]e^{-a(t-t_0)/\tau}. \tag{16}$$

Obviously, there is no regeneration process in the absence of healing, so that the cell is either dead or alive. These solutions demonstrate that each cell reaches its stationary state rather quickly, unless the relaxation time τ is very long. The stationary state is determined by the external load, tolerance of the cell, and the health status of the organism at $t-1$. This in turn determines the health status $\bar{x}(t)$ at time t, according to $\bar{x}(t) = N^{-1}\Sigma_k x_k(t)$.

We now consider the case that the organism suffers periodic stress of the following form:

$$f(t) = \frac{f_0}{2}(1 + \sin \Omega t), \tag{17}$$

with Ω being the frequency of the stress [8]. If the period $\mathcal{T}=2\pi/\Omega$ of the stress is sufficiently long compared with the relaxation time τ, the equation of motion (12) would still be valid, and we numerically integrate this equation in order to explore the time evolution of the system. We point out here that the results obtained via integration are in perfect agreement with those obtained from direct Monte Carlo simulations [9]. We consider the Gaussian distribution of the tolerance $\{h_i\}$ with unit mean $\bar{h}=1$ and standard deviation $\sigma=0.2$, in an organism of $N=10^4$ cells. Other distributions including the uniform distribution and the Weibull distribution have also been considered, only to give essentially the same results. Specifically, we use 20 different configurations of the tolerance distribution and set the relaxation time $\tau=5$ and the period of stress $\mathcal{T}=128$, with the time step $\Delta t=0.1$. These parameter values have been varied; this yields no qualitative difference as far as ac responses are concerned.

Figure 1 displays the health status of the organism for two values of peak stress f_0, with the period $\mathcal{T}=128$ or frequency $\Omega=0.049$. To help one to understand this figure, we briefly

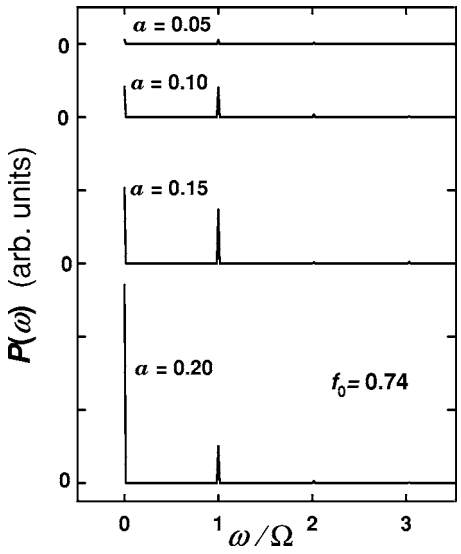

FIG. 2. Power spectrum $P(\omega)$ versus frequency ω (in units of the stress frequency Ω) at several values of the healing parameter a. The peak stress is given by $f_0=0.74$.

mention the behavior of the same system under constant stress [4]. The critical stress, above which breakdown occurs eventually, is given by $f_c=0.68$ at $a=0$ and increases slightly with a. When the stress f is much larger than f_c, the organism remains always unhealthy [characterized by small (steady-state) values of $\bar{x}$, say, less than 0.5, and mostly close to zero] even if a is increased. In the case that f is slightly above the critical stress f_c, the system becomes unhealthy at small values of a, as expected. As a is increased further, the system undergoes a transition to the healthy state (with the steady-state value of $\bar{x}$ larger than 0.5, mostly close to unity). The organism remains always healthy for stress smaller than f_c.

We now come back to Fig. 1. In the case that the peak value f_0 is smaller than f_c and there is no healing, the average fraction $\bar{x}$ of living cells decays stepwise and reaches a steady state, as shown in Fig. 1(a). When the healing parameter a is not zero, $\bar{x}$ grows with time for $f(t)$ being sufficiently small and decreases for $f(t)$ large enough. Accordingly, $\bar{x}$ becomes oscillating in time, while f oscillates between 0 and f_0. This oscillation becomes more dramatic when f_0 is larger than f_c, as shown in Fig. 1(b). When there is no healing (see the solid line in the figure), $\bar{x}$ decreases to zero. As a is raised from zero, the time average of $\bar{x}(t)$also increases, which can also be observed from the power spectrum $P(\omega)$, plotted in Figs. 2–4. The amplitude grows at first, reaches a peak, and then reduces, as a is increased. This can easily be understood by noting that $\bar{x}$ recovers more for small stress, as a becomes larger. However, at still larger values of a, $\bar{x}$ decreases less while the stress is large, resulting in a smaller amplitude. When the amplitude of $\bar{x}(t)$ is large, the behavior is apparently reminiscent of periodic synchronization, which emerges, for example, in systems of coupled oscillators [10].

To probe the time evolution in more detail, we compute the power spectrum $P(\omega)$ for several values of the healing parameter a. The result, obtained via the standard fast Fourier transform on 8192 data points, is shown in Fig. 2. It is observed that the power spectrum consists of sharp peaks at frequency $\omega=n\Omega$ with n integer—i.e., at the stress frequency and its harmonics. Paying attention to the peaks at $\omega=0$ and Ω, one notice that unlike $P(0)$, which grows monotonically with a, the power spectrum $P(\Omega)$ at the stress frequency exhibits nonmonotonic behavior as a is varied.

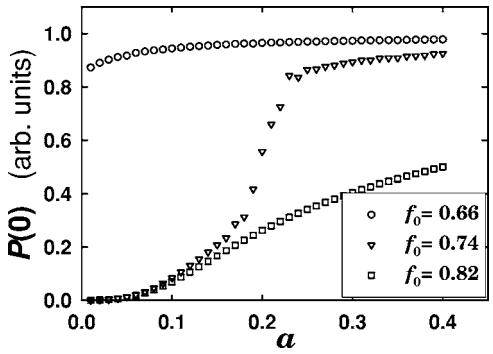

FIG. 3. Power spectrum at zero frequency $P(0)$ versus healing parameter a for three values of the peak stress f_0, shown in the legend. The stress frequency is $\Omega=0.049$.

These behaviors are manifested by the power spectrum $P(0)$ and $P(\Omega)$, plotted against the healing parameter a, in Figs. 3 and 4. Even though the stress is periodic, the state of the organism is either healthy or unhealthy at small values of a, depending on the peak stress f_0 (see Fig. 3). When f_0 is smaller than f_c, the organism is always in the healthy state and $P(0)$ increases only slightly with a. At values of f_0 slightly higher than f_c, the system goes, as a is increased, from the unhealthy state to the healthy one; this happens also for the organism under constant stress. At still higher values of f_0, there seems to be no transition and the system remains unhealthy. Figure 4 shows the power spectrum $P(\Omega)$ at the stress frequency for the same values of f_0 as in Fig. 3. It is obvious that $P(\Omega)$ at first increases with the healing parameter a and reaches a maximum at a moderate value of a. As a is raised further, $P(\Omega)$ then decreases, regardless of the peak stress f_0. Such nonmonotonic behavior in general characterizes resonance in dynamical systems [11–13], which has also been studied in some biological systems [14,15]. The resonancelike behavior here between the health status and

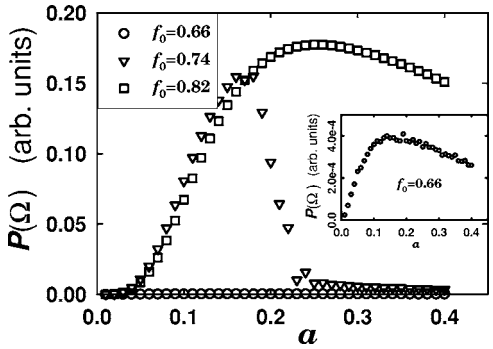

FIG. 4. Power spectrum at the stress frequency $P(\Omega)$ versus healing parameter a for the same values of f_0 and Ω as in Fig. 3. The inset shows the plot for $f_0=0.66$ in a finer scale.

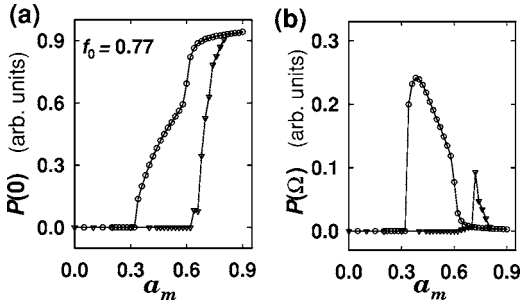

FIG. 5. Power spectrum (a) $P(0)$ at zero frequency and (b) $P(\Omega)$ at the stress frequency versus a_m, when the healing parameter is given by $a=a_m\bar{x}$ (∇) and by $a=a_m \tanh c\bar{x}$ with $c=2.5$ ($\bigcirc$). The peak stress is $f_0=0.77$, and other parameters are the same as those in Fig. 3. The lines are merely guides to the eye.

external stress arises from the interplay of the two time scales associated with cell regeneration (healing) and external stress (driving). Namely, the periodic evolution of the health status in response to the periodic external stress changes as the healing parameter is varied; in particular, the response follows more closely the external driving in the presence of an appropriate amount of healing, which we thus call *healing resonance*.

Heretofore we have assumed that the healing parameter a is independent of the health status $\bar{x}$. In the real situation, on the other hand, the health status is likely to affect the healing ability of the organism. Namely, as $\bar{x}$ reduces, presumably so does a. To investigate this possibility, we consider the case that the healing parameter a assumes a simple form. Specifically, we take (i) $a=a_m\bar{x}$ and (ii) $a=a_m \tanh c\bar{x}$ with a_m and c being constants. In either case, as $\bar{x}$ reduces to zero, the system loses healing ability ($a\to 0$). With these forms of the healing parameter, we carry out the same calculations as those for Figs. 3 and 4. Figure 5 presents the results for the power spectra (a) $P(0)$ at zero frequency and (b) $P(\Omega)$ at the stress frequency. Here the values $f_0=0.77$ and $c=2.5$ [in case (ii)] have been used, whereas other parameters are the same as those in Fig. 3. For small a_m, as expected, $\bar{x}(t)$ is observed to vanish eventually after transient oscillations and the zero-frequency power spectrum $P(0)$ remains zero, manifesting the complete failure of the organism. This behavior persists up to a threshold value of a_m, beyond which $P(0)$ grows rapidly from zero and $P(\Omega)$ exhibits the healing resonance behavior. The threshold value of a_m in general becomes larger as a decreases more rapidly with $\bar{x}$. Comparing the two cases (i) (down triangles) and (ii) (open circles) in Fig. 5, one may note that the reduction of a with $\bar{x}$ is faster in the former, leading to a larger threshold of a_m. The threshold also tends to grow larger as the peak stress f_0 is increased, which is not shown here.

Before moving to the next section, we digress a little to address the case of LLS, which may be more realistic in view of the connectivity between cells. Since the system with LLS is not analytically tractable, we resort to numerical simulations. For this purpose, we place $N\equiv L^2$ cells at sites of a square lattice of linear size L under periodic boundary conditions. The algorithm to simulate the load transfer is as follows: (i) Initially, all cells are alive, each characterized by spin $s=-1$ and subject to equal stress $f=F/L^2$. (ii) At each time step, the state of every cell gets updated according to the probability given by Eq. (4) or (5), depending on its present state. The order of update is determined at random. (iii) When a cell becomes dead ($s=+1$), its load is transferred to living (intact) cells at the nearest and second nearest sites—i.e., on the 2×2 square centered at the dead cell. Each neighbor receives an equal amount of the excess load. If there is no living cell on the first (2×2) square, the load is transferred to the living cells on the second (4×4) square and so on. If there is no living cell up to the tenth square of linear size 20, the load is shared by all living cells in the organism, each getting an equal amount. Obviously, this is just one of many possible ways to realize LLS and we have thus considered several other realizations of LLS, to find that the behavior of the system does not change qualitatively. (iv) A regenerated cell gets its load from nearby living cells in a similar manner: Each living neighbor chosen gives an equal amount of load to the regenerated cell, in such a way that the load on the new (regenerated) cell is equal to the average load of the chosen cells before the load transfer. (v) Measuring the health status $\bar{x}$ completes the time step, comprising one Monte Carlo sweep.

Using the same parameter values and the same distribution of tolerances as the previous GLS case, we have performed simulations, mostly in a system of size $L=64$. Figure 6(a) shows the average fraction $\bar{x}$ of living cells versus time t, obtained from Monte Carlo calculations for $f=0.61$ at $T=0$. The three curves describe the system with LLS for the healing parameter $a=0$ (solid line), 0.05 (dash-dotted line), and 0.2 (dash–double-dotted line), respectively. Also drawn, for comparison, is the dotted line representing the system with GLS for the same parameter values, which shows that the system does not break down. On the other hand, the system with LLS breaks down eventually, revealing that the system with LLS becomes weaker. With larger healing ability, however, the system resists the stress longer before the breakdown occurs and $\bar{x}$ still takes a finite value, again manifesting the healing effects. The system with LLS thus has just some quantitative differences compared with the case of GLS, which may be summarized as follows [9]: In comparison with the case of GLS, the value of f_c is smaller in the system with LLS at the same values of a and T. Also found is that better healing ability (i.e., a larger value of a) is required for the system with LLS to exhibit a transition to the healthy state. These trends remain unchanged regardless of the detailed scheme of LLS. We have also considered effects of shortcuts along which the load is transferred and found that as the number of pathways is increased, the critical stress of the system also increases and the system thus becomes stronger.

The qualitative responses of the system to periodic stress are also similar to those of the GLS system. Shown in Fig. 6(b) is the time evolution of $\bar{x}(t)$ for several values of the healing parameter: $a=0.05$ (dash-dotted line), 0.2 (dash–double-dotted line), and 0.5 (dashed line), respectively. The periodic stress is given by Eq. (17) with the peak stress $f_0=0.61$ and frequency $\Omega=0.049$. All data have been obtained from a single initial configuration of tolerances, which is the

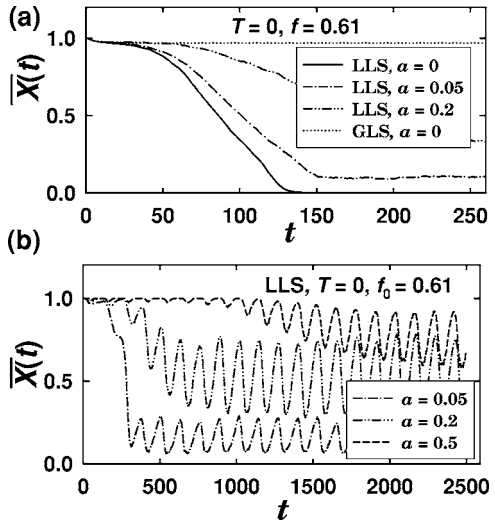

FIG. 6. (a) Average fraction $\bar{x}$ of living cells versus time t at $T=0$ and $f=0.61$, obtained from Monte Carlo calculations on a system with local load sharing. Cells are arranged to form a square lattice of size $L=64$, and the tolerance distribution is the same as that in Fig. 1. The three curves correspond to three different values of the healing parameter a, as shown in the legend. For comparison, the case of global load-sharing, with $a=0$ and other parameters being the same, is also shown (see the dotted line). Note that the stress is smaller than the critical stress $f_c=0.68$ of the global load-sharing system without noise. (b) Time evolution of the average fraction $\bar{x}$ of living cells under periodic stress, for several values of the healing parameter a shown in the legend. The stress is given by Eq. (17) with the peak stress $f_0=0.61$ and frequency $\Omega=0.049$. All data in (a) and (b) have been obtained from the same initial configuration of tolerances.

same as that used in (a). As the healing parameter a is raised, the time evolution of the system becomes similar to that of the GLS system in Fig. 1, with quantitative differences. Figure 7 shows the power spectrum $P(0)$ at zero frequency and $P(\Omega)$ at the stress frequency versus the healing parameter a. Note that the peak stress is again somewhat larger than the critical stress $f_c=0.57$ for the system under time-independent external stress. It is manifested that the healing resonance still appears even in the system with LLS.

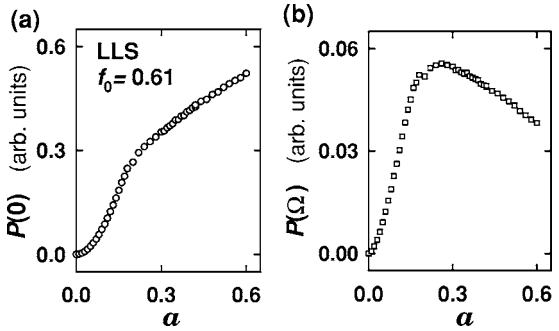

FIG. 7. Power spectrum (a) $P(0)$ at zero frequency and (b) $P(\Omega)$ at the stress frequency versus the healing parameter a, obtained from Monte Carlo calculations on the system in Fig. 6.

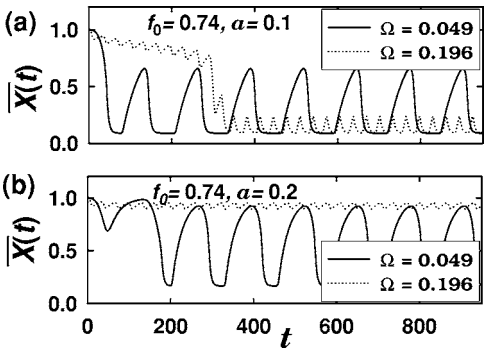

FIG. 8. Average fraction $\bar{x}(t)$ of living cells under stress given by Eq. (17) at two different values of a and Ω. The peak stress is given by $f_0=0.74$ while the values of $\bar{h}$ and σ are the same as those in Fig. 1. The healing parameter is given by $a=$ (a) 0.1 and (b) 0.2, respectively.

IV. STRESS AND HEALING

With the information in Sec. III, we examine the interplay between stress and healing, attending to the effects of periodicity of either stress or healing. We first examine the behavior of the system in Sec. III as the stress frequency is varied. Shown in Fig. 8 is the oscillatory time evolution of the health status depending on the stress frequency for two values of the healing parameter. The tolerance distribution is the same as that in Fig. 1—i.e., the values of $\bar{h}$ and σ are the same—and the peak stress is taken to be $f_0=0.74$.

At the low stress frequency ($\Omega=0.049$), the health status displays pronounced oscillations, without much regard to healing. As the stress frequency is increased, both the period and amplitude of oscillations of the health status are found to reduce significantly. In this high-frequency case ($\Omega=1.96$), the health status depends on healing in a crucial way: When the healing parameter a is small, the health status $\bar{x}(t)$, having mostly low values, may not get recovered sufficiently in the short (half) period and, accordingly, oscillates in the unhealthy state [see Fig. 8(a)]. For large a, on the other hand, Fig. 8(b) shows that the health status can get improved rapidly in the time interval and does not decrease much during the rest of the period. Thus $\bar{x}(t)$ oscillates in the healthy state.

This difference between the behaviors of Figs. 8(a) and 8(b) for $\Omega=1.96$ may also be understood in terms of the power spectrum. Plotting $P(0)$ for $f_0=0.74$ at this frequency ($\Omega=1.96$), which is similar to Fig. 3 and thus not shown here, we observe a transition from the unhealthy to the healthy states as a is increased. In this manner, the health status depends on the stress frequency and the healing parameter as well as the peak stress, when the peak stress is a bit larger than f_c. It is of particular interest to note that stress of higher (lower) frequency is better for health when healing is more (less) active.

We next consider the case that healing (rather than stress) varies periodically in time. Such periodic healing, related to those effects of periodic stress, is commonly observed in human life. For example, healing may be affected by medical treatments or other activities, which are periodic in time. We thus consider an organism under constant stress f, with the healing parameter of the form

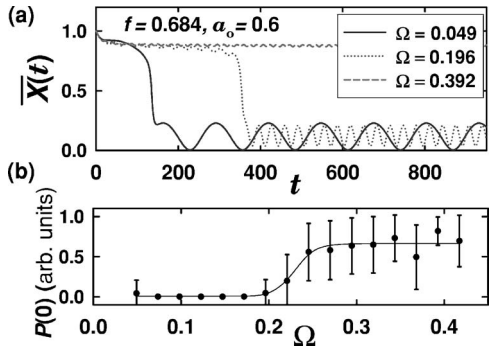

FIG. 9. (a) Average fraction $\bar{x}(t)$ under constant stress $f=0.684$ with the time-dependent healing parameter $a(t)$ given by Eq. (18). The peak value a_0 is taken to be 0.6 while the healing frequency Ω is 0.049 (solid line), 0.196 (dotted line), and 0.392 (dashed line). (b) Power spectrum at zero frequency, $P(0)$, versus the healing frequency Ω, exhibiting a transition from the unhealthy state to the healthy one. The error bars have been estimated by the standard deviation, and the line is merely a guide to the eye. The values of a_0 and f are the same as in (a).

$$a(t) = \frac{a_0}{2}(1 + \sin \Omega t), \tag{18}$$

and exhibit the resulting behavior in Fig. 9.

Figure 9(a) displays the health status $\bar{x}(t)$ at several values of the healing frequency Ω, with (constant) stress $f=0.684$ and peak healing parameter $a_0=0.6$. The organism is observed to be in the unhealthy state at lower two frequencies, while it is in the healthy state at the highest frequency. Plotting the power spectrum $P(0)$ at zero frequency against the healing frequency Ω, we make clear that the system exhibits a transition from the unhealthy state to the healthy one as Ω is increased beyond a critical value Ω_c [see Fig. 9(b)]. When f is slightly above f_c and the healing frequency Ω is high enough, the healing parameter $a(t)$ grows from the minimum before $\bar{x}$ decreases much, resulting in the healthy state. This behavior disappears when f becomes far larger than f_c; this corresponds simply to the situation that the organism may not be restored to health by medical treatment if stress is too large.

Our result that the health status changes rather abruptly with the healing frequency indicates, in part, that the frequency of treatment should be adjusted to the optimum in medication: In general a high-frequency treatment is more effective for the recovery of health, as shown in Fig. 9. However, in view of the price and possible side effects, it is desirable to keep the treatment frequency to the minimum. Figure 9(b) suggests that these conflicting circumstances may be resolved by taking the optimal frequency Ω_o to be slightly above the critical value Ω_c—e.g., $\Omega_o \approx 0.25$ in this case.

V. SUMMARY

We have applied the dynamic model for failures to a living organism under periodic stress. Without healing, the average fraction $\bar{x}$ of intact cells, dubbed the health status, either decays stepwise to zero or to a constant value far from zero, depending on the peak value of the stress. When the healing parameter a is introduced and increased from zero, the health status $\bar{x}$ exhibits oscillating behavior, resembling periodic synchronization. It is observed that the power spectrum at the stress frequency increases at first with a raised, then decreases, which manifests healing resonance. We have also investigated the effects of stress frequency. When the peak stress f_0 is a bit larger than the critical value f_c, the health status is found to depend on the stress frequency and the healing parameter, as well as the peak stress. Here arises an interesting interplay of healing and stress frequency: When healing is not active, the system tends to resist low-frequency stress better than a high-frequency one. As healing becomes active, on the other hand, the stress of high frequency becomes more tolerable than the low-frequency one, and the system may remain healthy if the stress frequency is sufficiently high. Finally, we have studied the time evolution of an organism in the case that the healing parameter varies periodically with time and the stress f is slightly above f_c. It has been found that the system, under stress slightly above f_c, exhibits a transition from the unhealthy state to the healthy state as the healing frequency is increased. Such dependence of the health status on the healing frequency gives interesting implications for medication, with regard to the optimal frequency of treatment.

ACKNOWLEDGMENTS

This work was supported by MOST (KOSEF) through National Core Research Center for Systems Bio-dynamics (M.Y.C.) and by the 2005 Research Fund of the University of Ulsan (B.G.Y.). M.Y.C. also acknowledges a visitor grant from the CNRS, France, and thanks the Laboratoire de Physique Théorique, Strasbourg, for its kind hospitality during his stay.

[1] For a review, see, e.g., R. da Silveira, Am. J. Phys. **67**, 1177 (1999); B. K. Charkrabarti and L. G. Benguigui, *Statistical Physics of Fracture and Breakdown in Disordered Systems* (Clarendon, Oxford, 1997).

[2] J. V. Andersen, D. Sornette, and K.-T. Leung, Phys. Rev. Lett. **78**, 2140 (1997); S. D. Zhang, Phys. Rev. E **59**, 1589 (1999); S. Roux, *ibid.* **62**, 6164 (2000); W. I. Newman and S. L. Phoenix, *ibid.* **63**, 021507 (2001).

[3] L. Moral, Y. Moreno, J. B. Gomez, and A. F. Pacheco, Phys. Rev. E **63**, 066106 (2001); R. Scorretti, S. Ciliberto, and A. Guarino, Europhys. Lett. **55**, 626 (2001); S. Pradhan, P. Bhattacharyya, and B. K. Chakrabarti, Phys. Rev. E **66**, 016116 (2002); M. Y. Choi, J. Choi, and B.-G. Yoon, Europhys. Lett. **66**, 62 (2004); B. J. Kim, *ibid.* **66**, 819 (2004).

[4] J. Choi, M. Y. Choi, and B.-G. Yoon, Europhys. Lett. **71**, 501 (2005).

[5] See, e.g., A. E. Butler, J. Janson, S. Bonner-Weir, R. Ritzel, R. A. Rizza, and P. C. Butler, Diabetes **52**, 102 (2003); F. Ashcroft and P. Rorsman, Hum. Mol. Genet. **13**, R21 (2004). For some modeling, see, e.g., B. F. de Blasio, P. Bak, F. Pociot, A. E. Karlsen, and J. Nerup, Diabetes **48**, 1677 (1999); M. V. Risbud and R. R. Bhonde, Diabetes Res. Clin. Pract. **58**, 155 (2002).

[6] See, e.g., *Alzheimer's Disease*, edited by R. D. Terry, R. Katzman, and K. Bick (Raven, New York, 1994); I. Vincent, G. Jicha, M. Rosado, and D. W. Dickson, J. Neurosci. **17**, 3588 (1997) and references therein.

[7] See, e.g., C. Kamp and S. Bornholdt, Proc. R. Soc. London, Ser. B **269**, 2035 (2002) and references therein.

[8] Other forms of periodic stress have also been considered and found to give qualitatively the same results as described here, unless the amplitude of the ac component is too small.

[9] B.-G. Yoon, J. Choi, and M. Y. Choi, J. Korean Phys. Soc. **47**, 1053 (2005)

[10] M. Y. Choi, Y. W. Kim, and D. C. Hong, Phys. Rev. E **49**, 3825 (1994); Y. Shim, H. Hong, and M. Y. Choi, *ibid.* **65**, 036114 (2002); S. Nagano, *ibid.* **67**, 056215 (2003).

[11] See, e.g., L. Gammaitoni, P. Hänggi, P. Jung, and F. Marchesoni, Rev. Mod. Phys. **70**, 223 (1998) and references therein.

[12] M. Acharyya, Phys. Rev. E **59**, 218 (1999); K.-T. Leung and Z. Néda, *ibid.* **59**, 2730 (1999); B. J. Kim, P. Minnhagen, H. J. Kim, M. Y. Choi, and G. S. Jeon, Europhys. Lett. **56**, 333 (2001).

[13] H. Hong, M. Y. Choi, K. Park, B.-G. Yoon, and K. S. Soh, Phys. Rev. E **60**, 4014 (1999); G. S. Jeon, J. S. Lim, H. J. Kim, and M. Y. Choi, Phys. Rev. B **66**, 024511 (2002).

[14] W. Sung and P. J. Park, Physica A **254**, 62 (1998); C. H. Chang and T. Y. Tsong, Phys. Rev. E **69**, 021914 (2004); J. Dunkel, S. Hilbert, L. Schimansky-Geier, and P. Hänggi, Phys. Rev. E **69**, 056118 (2004).

[15] F. G. Zeng, G. J. Fu, and R. Morse, Brain Res. **869**, 251 (2000); L. M. Ward, A. Neiman, and F. Moss, Biol. Cybern. **87**, 91 (2002); K. Kitajo, D. Nozaki, L. M. Ward, and Y. Yamamoto, Phys. Rev. Lett. **90**, 218103 (2003); F. Moss, L. M. Ward, and W. G. Sannita, Clin. Neurophysiol. **115**, 267 (2004).